Scientific Review Engineering and Environmental Sciences (2023), 32 (1), 34–52

Sci. Rev. Eng. Env. Sci. (2023), 32 (1) https://srees.sggw.edu.pl

ISSN 1732-9353 (suspended) eISSN 2543-7496 DOI 10.22630/srees.4478

Received: 26.09.2022
Accepted: 01.12.2022

Rachid BAKHTI[1]✉

Baizid BENAHMED[2] https://orcid.org/0000-0003-4924-0059

Abdelghani LAIB[3]

[1, 3]University of Bouira, Faculty of Science and Applied Science, Algeria
[2]University of Djelfa, Development Laboratory in Mechanics and Materials, Algeria

Investigation for stress–strain curves of the plastic damage model for concrete

Keywords: plastic damage model, Barcelona model, concrete structures, nonlinear finite element method, stress–strain correlations

Introduction

Concrete is a material conventionally used for construction that is of major importance in the field of civil engineering. Mastering concrete structural design involves full control of the finite element analysis, which required using an appropriate numerical constitutive law to describe the real behavior of the concrete material. Several numerical constitutive laws were provided in the last few decades in order to describe the behavior of concrete. The linear and nonlinear elastic models are the simplest constitutive laws for describing the behavior of concrete. This category of models presumes a linear/nonlinear relationship between the stresses and the strains for the tension and the compression cases, the correlation between stresses and strains is governed by Hooke's law for the linear case, what is more, this category of models is characterized by elastically returning to the "unloaded" state after loading. This kind of model is quite accurate and sufficient to forecast

✉r.bakhti@univ-bouira.dz

the behavior of concrete for minor strain values, but it shows an important error margin when the strain values are significant. To overcome this issue a second category of models was developed using the plasticity theory in order to improve the accuracy of the outcomes for significant strain values. For the plasticity models, various constitutive laws were developed specifically for concrete, such as Ottosen (1977), and Menetrey and Willam (1995), where multiple modifications into the plasticity theory were provided in order to compute the strain and the stress. In addition, Han and Chen (1986), Dvorkin, Cuitińo and Gioia (1989) advised using the Drucker and Prager's yield function as a potential function to estimate the plastic strain, in the same manner, Vermeer and De Borst (1984) employed the constitutive equation of Mohr and Coulomb to provide a new potential function, in which substituting the internal friction angle with the dilatancy angle was suggested. The category of plasticity models can perfectly address small and large strains, but, unfortunately, this category of models cannot handle the concrete degradation which provides a large margin of error specifically after the peak point; furthermore, the concrete behavior is not the same for tension and compression cases. As recapitulation, the use of plasticity models to presume the behavior of concrete structures provides inaccurate outcomes, especially after the peak point. Several papers (Lubliner, Oliver, Oller & Ońate, 1989; Paliwal, Hammi, Moser & Horstemeyer, 2017; Poliotti & Bairán, 2019; Bhartiya, Sahoo & Verma, 2021; Xiao, Chen, Zhou, Leng & Xia, 2021; Liu, Zhang, Zhao, Wu & Guo, 2022; Lu, Meng, Zhou, Wang & Du, 2022) combine the damage of concrete with the plasticity theory to provide yet another category of models referred to as plastic damage models. One of the most innovative models in this category was developed by Lubliner et al. (1989) called the damage plastic model (DPM) also known as the Barcelona model. This model was upgraded by Lee and Fenves (1998) to address the cyclic loading. The recent form of this model was used by Javanmardi and Maheri (2019) to predict the crack propagation paths. Furthermore, Ahmed, Voyiadjis and Park (2020) suggested a new finite element implementation of this model through a novel stress decomposition. The new form of this model (Lee & Fenves, 1998) was implemented in the commercial finite element code ABAQUS under the name of concrete damaged plasticity model (CDPM). The CDPM has been widely used in various research papers, such as the work of Silva, Gamage and Fawzia (2019) where they used it to simulate the concrete damage. Likewise, Ren, Sneed, Yang and He (2015) used CDPM in the numerical simulation of prestressed precast concrete bridge deck panels. In addition, Othman and Marzouk (2018) used the CDPM to simulate ultra-high-performance fiber reinforced concrete material under impact loading rates at different damage stages. In the same manner, Meng, Yang and Yang (2022) used ABAQUS to evaluate the damage evolution of double--tube concrete column under axial force.

Various parameters are required to simulate the behavior of concrete using CDPM; the stress–inelastic strain diagram for compression and tension cases, the damage parameters evolution for compression and tension cases, the ratio of the second stress invariants on tensile and compressive meridians, the eccentricity, the ratio of biaxial compressive yield stress to uniaxial compressive yield stress, and the dilation angle. Minh, Khatir, Wahab and Cuong-Le (2021) suggested multiple enhancements of CDPM in order to eliminate several parameters where the softening phase in the compressive stress–strain curve has been modified and each of the tensile damage variables and the compressive damage variables was evaluated through an exponential function. To avoid those parameters, a local computer program was developed by the author called Concrete v. 2.0, where only the concrete strength is required for modeling concrete structures (Bakhti, Benahmed, Laib & Alfach, 2022).

This work examined the effect of the hardening function used in the finite element implementation of DPM on the final outcomes by comparing the generated stress–strain diagrams with the analytical solutions of Lubliner and also with other formulas suggested, respectively, by Desayi and Krishnan (1964) and Krätzig and Pölling (2004) for the compression case, and Thorenfeldt (1987) for the tension case. The outcomes of the Barcelona model presented in this paper are calculated by Concrete v. 2.0 using the methodology proposed in Bakhti et al. (2022), where the Lubliner's formulas (Lubliner et al., 1989) have been selected as a hardening function in the finite element implementation of DPM. For the compression case, this paper compared the stress–strain diagrams generated according to the Barcelona model with the stress–strain diagrams of Desayi and Krishnan (1964), Lubliner et al. (1989), and Krätzig and Pölling (2004). For the tension case, the stress–strain curves were compared with the stress–strain curves of Thorenfeldt et al. (1987) and Lubliner et al. (1989). This study helped select five values of concrete strengths, namely: 20 MPa, 25 MPa, 30 MPa, 35 MPa and 40 MPa.

Plastic damage model for concrete

The main concept of DPM is to substitute the hardening variable in the overall form of classical plasticity with the plastic damage variable. The value of the damage variable varies between zero and one, where the zero value represents the undamaged concrete and the value of one represents the totally damaged concrete with a full loss of cohesion. The fundamental equations of this model are as follows.

a) For the yield function

$$F = \frac{1}{1-\alpha}\left(3\alpha p + \sqrt{3}J + \beta\left\langle \sigma_{max}\right\rangle - \gamma\left\langle -\sigma_{max}\right\rangle\right) - c, \tag{1}$$

with α, β and γ are dimensionless parameters given by:

$$\alpha = \frac{\left(\frac{f_{b0}}{f_{c0}} - 1\right)}{\left(2\frac{f_{b0}}{f_{c0}} - 1\right)}, \tag{2}$$

$$\beta = R(1-\alpha) - (1+\alpha) \text{ with } R = \frac{f_{c0}}{f_{t0}}, \tag{3}$$

$$\gamma = 3(1 - r_{oct}^{max})/(2r_{oct}^{max} - 1), \tag{4}$$

where: p – mean total stress, J – deviatoric stress, σ_{max} – maximum principal effective stress, c – cohesion, $\frac{f_{b0}}{f_{c0}}$ – ratio of biaxial and uniaxial compressive yield strengths. In SIMULIA (2010), the default value is 1.16, f_{t0} – initial uniaxial tensile yield stress, r_{oct}^{max} – constant takes a value of 0.65, according to Oller, Ońate, Oliver and Lubliner (1990), $\langle X \rangle$ – Macaulay's bracket and takes the form: $\langle \pm X \rangle = \frac{X \pm |X|}{2}$.

b) For the potential function

Lubliner et al. (1989) suggested a non-associated potential plastic flow. The potential function takes the same form as the classic Mohr–Coulomb constitutive equation with replacing the friction angle with the dilation angle. The potential function suggested by Lubliner et al. (1989) takes the following form:

$$G = p \sin\psi + J\left(\cos\theta - \frac{\sin\theta \sin\psi}{\sqrt{3}}\right), \tag{5}$$

where: p – mean total stress, ψ – dilation angle, J – deviatoric stress, θ – lode angle.

The second form of this model was developed by Lee and Fenves (1998) to address the dynamic loading where the following modifications were proposed, as follows.

a) For the yield function substituting cohesion c by effective compressive cohesion stress $\overline{\sigma_c}$, or new formulas for β and γ parameters, given as:

$$\beta = \frac{\overline{\sigma_c}}{\overline{\sigma_t}}(1-\alpha)-(1+\alpha), \tag{6}$$

$$\gamma = \frac{3(1-K_c)}{2K_c-1}, \tag{7}$$

where: $\overline{\sigma_c}$ – effective compressive cohesion stress, $\overline{\sigma_t}$ – effective tensile cohesion stress, K_c – ratio of second stress invariants on tensile and compressive meridians.

As a result, the second form of the yield function suggested by Lee and Fenves (1998) is written as:

$$F = \frac{1}{1-\alpha}\left(3\alpha\, p+\sqrt{3}J+\beta\langle\sigma_{\max}\rangle-\gamma\langle-\sigma_{\max}\rangle\right)-\overline{\sigma_c}; \tag{8}$$

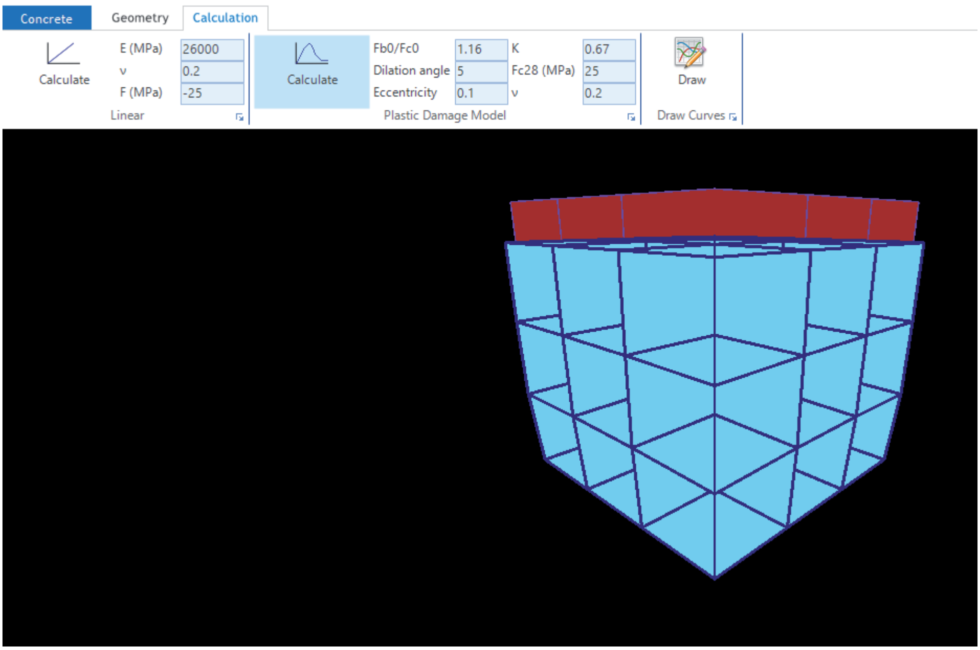

FIGURE 1. Modeling cubical concrete sample using Concrete v. 2.0 (dimensions: 300 × 300 × × 300 mm)

Source: own work.

b) For the potential function, suggested by Lee and Fenves (1998), takes the form:

$$G = \sqrt{(\varepsilon \sigma_{t0} \tan\psi)^2 + 3J^2} + p \tan\psi, \tag{9}$$

where: ε – flow potential eccentricity – 0.1 in SIMULIA (2010), σ_{t0} – uniaxial tensile stress at failure.

Bakhti et al. (2022) developed a finite element program under the name Concrete v. 2.0 to model concrete behavior using DPM as a constitutive model and object-oriented programming paradigm (OOP) as a coding technique. All DPM curves presented in this paper were calculated by Concrete v. 2.0 for a cubical element with dimensions: 300 × 300 × 300 mm and by hiring the 8 nodes cubical element to generate 27 elements (Fig. 1).

Stress–strain correlations

Lubliner's stress–strain correlation

In 1989, Lubliner et al. (1989) suggested general correlations between the compressive and tensile stresses and the inelastic strain. Those correlations are used by Bakhti et al. (2022) as a hardening function in the finite implementation of DPM. According to the suggested correlations, the compressive and tensile stresses depend on the values of the coefficients a_c, a_t, b_c and b_t. The values of these coefficients were evaluated by Bakhti et al. (2022) according to the CEB-FIP Model Code recommendations (Comité euro-international du béton & Fédération internationale du béton [CEB-FIP], 2010) and presented in Tables 1 and 2. The stress–strain correlations suggested by Lubliner for tension and compression take the following forms:

$$\begin{cases} \sigma_c = f_{c0}\left[(1+a_c)e^{-b_c\varepsilon_c^{in}} - a_c e^{-2b_c\varepsilon_c^{in}}\right] \\ \sigma_t = f_{t0}\left[(1+a_t)e^{-b_t\varepsilon_t^{ck}} - a_t e^{-2b_t\varepsilon_t^{ck}}\right] \end{cases}. \tag{10}$$

For the stress–strain correlations, Bakhti et al. (2022) divided these curves into two parts for the compression and tension cases as shown in Figure 2. The first part represents the linear segment where the stress is evaluated according to Hooke's law. The second one represents the non-linear part where the stress is evaluated according to Lubliner's formulas.

TABLE 1. Values of coefficients a_c, a_t, b_c and b_t for different concrete strength – Part 1

Coefficient	f_{ck} [MPa]						
	12	16	20	25	30	35	40
a_c	7.873	7.873	7.873	7.873	7.873	7.873	7.873
a_t	637.077	636.468	638.065	641.894	646.876	652.439	658.218
b_c	1.00	1.00	1.00	1.00	1.00	1.00	1.00
b_t	6 122.778	6 059.292	6 107.316	6 240.193	6 412.655	6 604.052	6 803.804

Source: own work.

TABLE 2. Values of coefficients a_c, a_t, b_c and b_t for different concrete strength – Part 2

Coefficient	f_{ck} [MPa]						
	45	50	55	60	70	80	90
a_c	7.873	7.873	7.873	7.873	7.873	7.873	7.873
a_t	663.972	669.533	674.783	679.639	687.945	698.146	794.836
b_c	1.00	1.00	1.00	1.00	1.00	1.00	1.00
b_t	7 005.913	7 206.661	7 403.612	7 595.106	7 957.263	8 334.567	9 769.134

Source: own work.

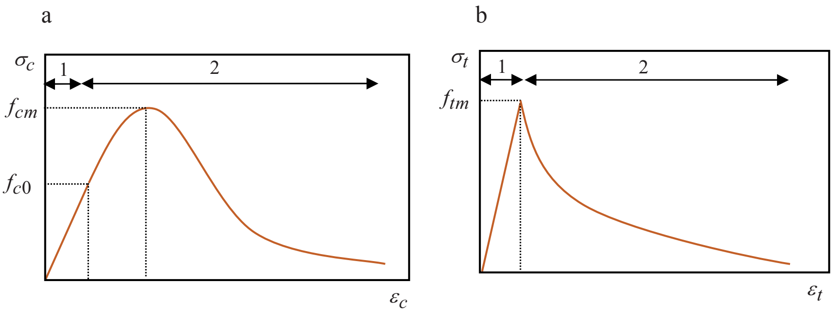

FIGURE 2. Decomposition of stress–strain curve in compression (a) and tension (b)

Source: own work.

Desayi and Krishnan's correlation

Using a series of experimental tests, several researches attempted to provide correlations between the stress and strain for both cases of compression and tension where the experimental outcomes are used to develop functions that can describe the material behavior. The simplest relationship was developed by Desayi and Krishnan (1964) that takes the following form:

$$\sigma = \frac{E\varepsilon}{1+\left(\frac{\varepsilon}{\varepsilon_p}\right)^2}, \tag{11}$$

where: σ, ε – stress and strain tensors, E – Young's modulus, ε_p – strain at peak stress.

Krätzig and Pölling's correlation

This approach was adopted in the multiple research work to evaluate the compressive stress–strain diagrams. For instance, Alfarah, López-Almansa and Oller (2017) used the correlations of Krätzig and Pölling (2004) in their algorithm to auto-evaluate the stress–strain diagrams in ABAQUS. In this approach, the stress–strain curve is divided into three parts as shown in Figure 3, where the stress values are evaluated by:

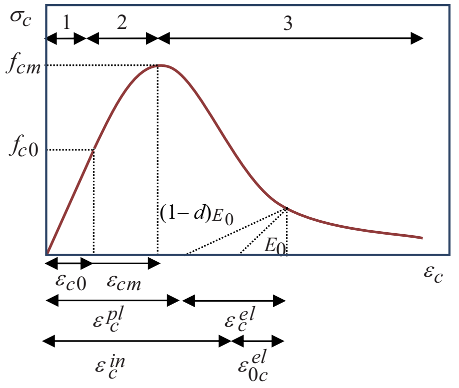

FIGURE 3. Krätzig's decomposition of the compressive stress–strain curve

Source: own work.

– first part (linear till f_{c0}):

$$\sigma_{c(1)} = E_0 \varepsilon_c, \tag{12}$$

– second part (ascending between f_{c0} and f_{cm}):

$$\sigma_{c(2)} = \frac{E_{ci}\frac{\varepsilon_c}{f_{cm}} - \left(\frac{\varepsilon_c}{\varepsilon_{cm}}\right)^2}{1 + \left(E_{ci}\frac{\varepsilon_{cm}}{f_{cm}} - 2\right)\frac{\varepsilon_c}{\varepsilon_{cm}}} f_{cm}, \tag{13}$$

– third part (descending), given by:

$$\sigma_{c(3)} = \left(\frac{2 + \gamma_c f_{cm} \varepsilon_{cm}}{2 f_{cm}} - \gamma_c \varepsilon_c + \frac{\varepsilon_c^2 \gamma_c}{2 \varepsilon_{cm}}\right)^{-1} \text{ with } \gamma_c = \frac{\pi^2 f_{cm} \varepsilon_{cm}}{2\left[\frac{G_{ch}}{L_{eq}} - 0.5 f_{cm}\left(\varepsilon_{cm}(1-b) + b\frac{f_{cm}}{E_0}\right)\right]^2}; \; b = \frac{\varepsilon_c^{pl}}{\varepsilon_c^{in}}, \tag{14}$$

where: f_{c0} – compressive stress that correspond to zero crushing, f_{cm} – peak compressive stress, ε_{cm} – strain at the peak compressive stress, E_0 – undamaged modulus of deformation, E_{ci} – initial tangent modulus of deformation of concrete, G_{ch} – crushing energy per unit area, L_{eq} – mesh size (characteristic length), ε_c^{pl} – compressive plastic strain, ε_c^{in} – compressive inelastic strain.

Thorenfeldt's correlation

According to the Thorenfeldt's approach (Thorenfeldt, 1987), the tensile stress–strain curve can be divided into two parts. In the first part (till the peak point), the stress value is evaluated according to the Hooke's law. In the second part, the tensile stress is calculated in accordance with the following formula:

$$\sigma_t = f_{tm}\left(\frac{\varepsilon_{tm}}{\varepsilon_t}\right)^{(0.7+1,000\varepsilon_t)}, \tag{15}$$

where: f_{tm} – peak tensile stress, ε_{tm} – strain at the peak tensile stress.

Comparing the stress–strain curves of the barcelona model and several analytical correlations

Five values of concrete strengths are chosen to examine the outcomes of the Barcelona model compared to three stress–strain correlations for the compression case, namely: Desayi and Krishnan (1964), Lubliner et al. (1989), and Krätzig and Pölling (2004), and two stress–strain correlations for the tension case, that is: Thorenfeldt et al. (1987) and Lubliner et al. (1989). The selected values of concrete strengths are: 20 MPa, 25 MPa, 30 MPa, 35 MPa and 40 MPa. Each of Young's moduli and the strain value at peak stress that needed to calculate the stress value according to Desayi and Krishnan's correlation (Desayi & Krishnan, 1964) for each value of concrete strength are delivered in Table 3.

For Krätzig and Pölling's correlation (Krätzig & Pölling 2004), all curves are calculated the based on the mesh size of 300 mm. In addition, we used the model code recommendations (CEB-FIP, 2010) to calculate the following parameters:

– initial tangent modulus of deformation of concrete $E_{ci} = 10\,000\, f_{cm}^{1/3}$, (16)

– undamaged modulus of deformation $E_0 = E_{ci}\left(0.8 + 0.2\frac{f_{cm}}{88}\right)$, (17)

– compressive stress that corresponds to zero crushing $f_{c0} = 0.4\, f_{cm}$, (18)

– value of the strain at the peak stress $\varepsilon_{cm} = 0.5\, f_{cm}^{0.31} \leq 2.8 \cdot 10^{-3}$, (19)

– crushing/fracture energy $G_{ch} = \left(\frac{f_{cm}}{f_{tm}}\right)^2 G_F$ [N·mm^{-1}], where $G_F = 0.073 f_{cm}^{0.18}$. (20)

Table 4 summarizes the values of the peak tensile stress and the strain at the peak tensile stress for each value of concrete strength that are required to evaluate the stress value according to Thorenfeldt's correlation. For Lubliner's correlations, we used the values of coefficients a_c, a_t, b_c and b_t that were calculated by Bakhti et al. (2022) and are presented in Tables 1 and 2. Moreover, according to this approach, the compressive and tensile stress–strain curves were divided into two parts. The first one represents the linear segment where the stress is evaluated according to Hooke's law. The second one represents the non-linear part where the stress is evaluated according to Lubliner's formulas.

For the compression case and according to Figures 4–8, the following observations can be outlined:

– The curves of the Barcelona model that were generated by Concrete v. 2.0 are completely in harmony with the stress–strain curve generated, according to the Lubliner's formula; this observation can be justified by the fact that the hardening function used in the implementation of DPM is identical to Lubliner's formulas.
– For the concrete strengths less than 25 MPa, the outcomes of the Barcelona model calculated using Concrete v. 2.0 are partly consistent with the stress–strain curve generated according to the Krätzig's formula. For values more than 25 MPa and using the Krätzig decomposition (Fig. 3), we observed that the curves of the Barcelona model diverge from the Krätzig's curve depending on the concrete strengths, especially in the third part.
– Using the Krätzig decomposition (Fig. 3), the outcomes of the Barcelona model are partly consistent with the stress–strain curve generated according to the Desayi's formula in the first and the second part (Fig. 3). As for the third part, the difference between both curves is significant.

TABLE 3. Input data of Desayi and Krishnan's curve

f_{cm} [MPa]	ε_p (×10^{-3}) [-]	E [MPa]
20	1.8	22 890
25	1.9	26 130
30	2	29 910
35	2.1	32 890
40	2.2	35 940

Source: own work.

TABLE 4. Input data of Thorenfeldt's curve

f_{cm} [MPa]	ε_{tm} (×10^{-4}) [-]	f_{tm} [MPa]
20	0.68	1.58
25	0.79	1.99
30	0.87	2.37
35	0.93	2.71
40	0.98	3.04

Source: own work.

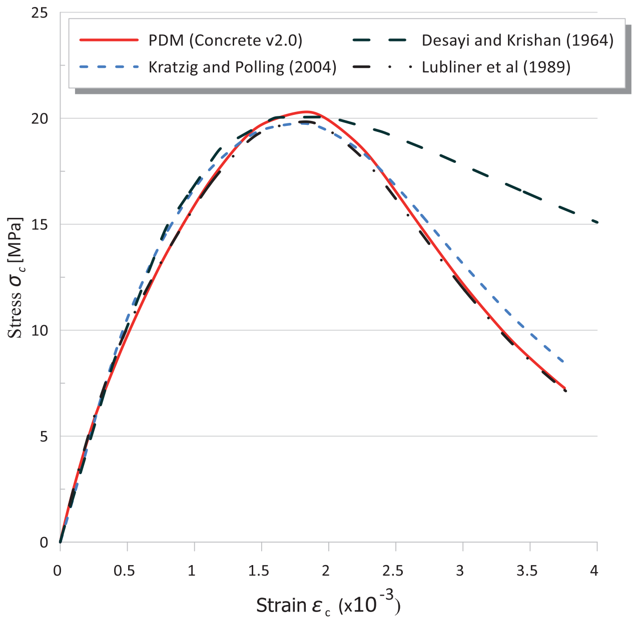

FIGURE 4. Compressive stress–strain curve for f_{cm} = 20 MPa
Source: own work.

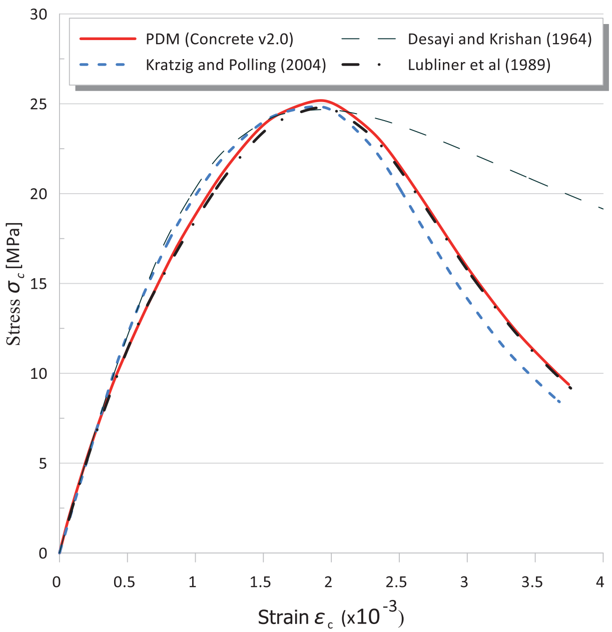

FIGURE 5. Compressive stress–strain curve for f_{cm} = 25 MPa
Source: own work.

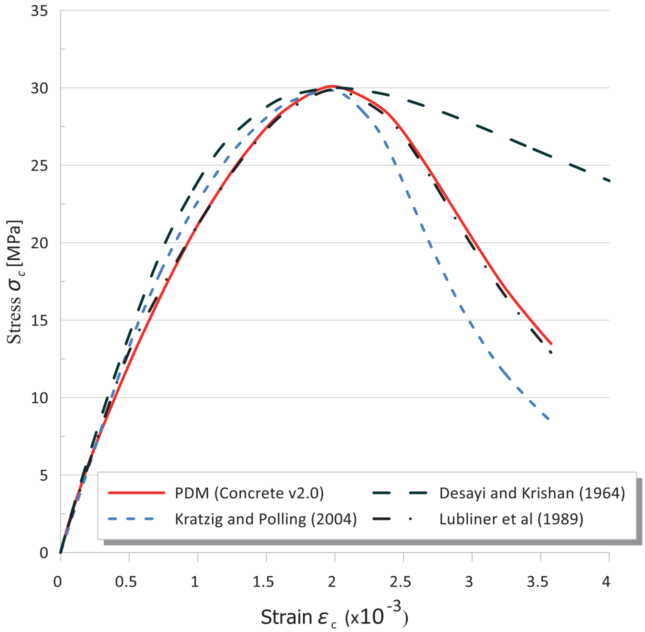

FIGURE 6. Compressive stress–strain curve for f_{cm} = 30 MPa
Source: own work.

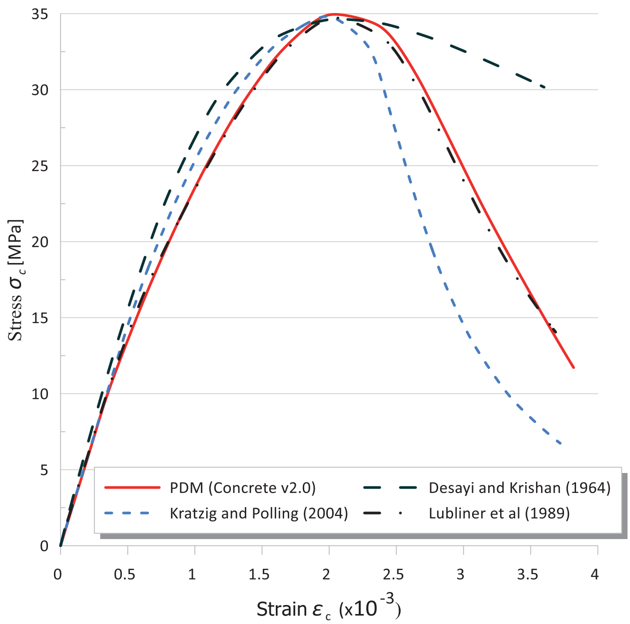

FIGURE 7. Compressive stress–strain curve for f_{cm} = 35 MPa
Source: own work.

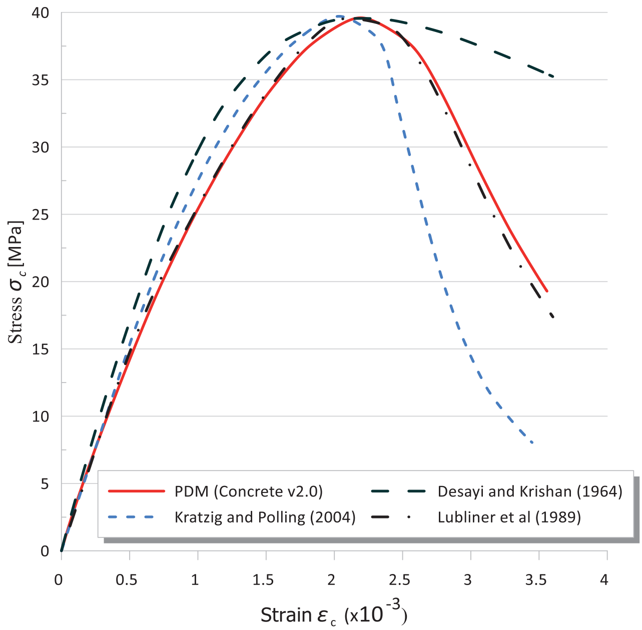

FIGURE 8. Compressive stress–strain curve for f_{cm} = 40 MPa
Source: own work.

For the tension case and in terms of Figures 9–13, the following notes can be made:

– The outcomes of the Barcelona model are consistent with the stress-strain curve generated according to the Lubliner's formula, which can be justified by the adopted hardening function that is identical to Lubliner's formulas.
– Using the decomposition of the tensile stress–strain curve that is illustrated in Figure 2b, the tensile curves of the Barcelona model are entirely consistent with the stress–strain curve generated according to the Thorenfeldt's formula in the first part. As for the second part, the Barcelona model gives results that are partly similar to the Thorenfeldt's formula.

Those observations are based mainly on the fact that the compressive and tensile stress–strain curves of the Barcelona model are calculated according to Lubliner's correlations that are used as a hardening function in our finite element implementation. To address another correlation, a simple modification in the finite element implementation of DPM will be required through re-computing, the derivative of the yield function with respect of stresses, the derivative of the yield function with respect of the inelastic compression strain.

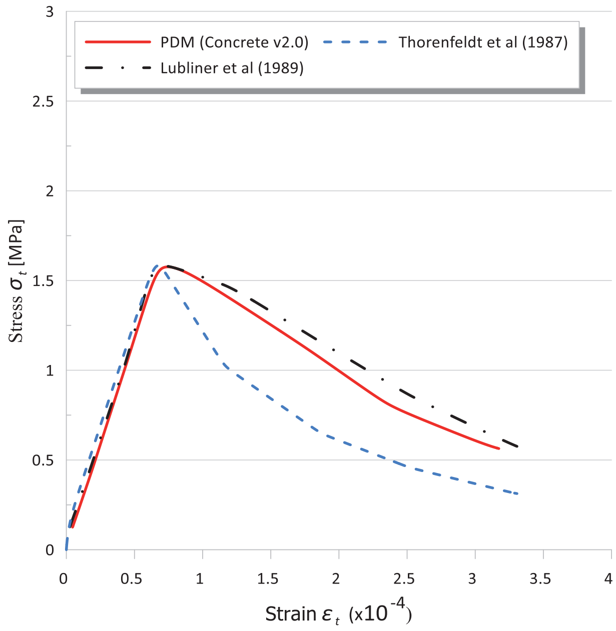

FIGURE 9. Tensile stress–strain curve for f_{cm} = 20 MPa (f_{tm} = 1.58 MPa)
Source: own work.

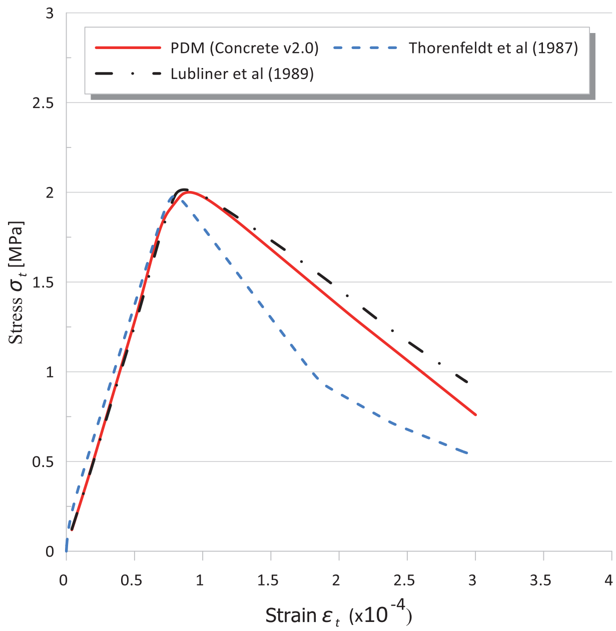

FIGURE 10. Tensile stress–strain curve for f_{cm} = 25 MPa (f_{tm} = 1.99 MPa)
Source: own work.

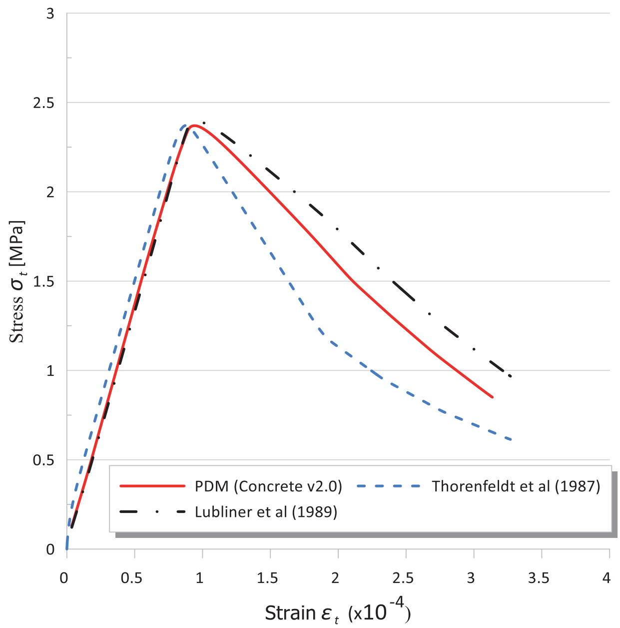

FIGURE 11. Tensile stress–strain curve for f_{cm} = 30 MPa (f_{tm} = 2.37 MPa)
Source: own work.

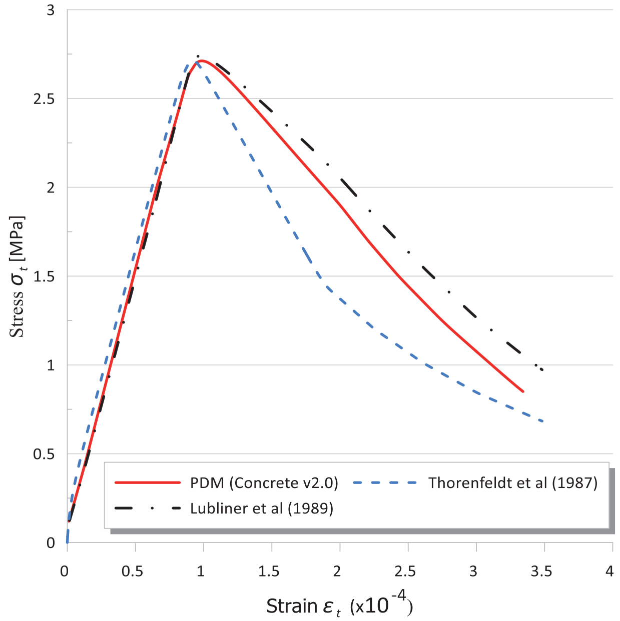

FIGURE 12. Tensile stress–strain curve for f_{cm} = 35 MPa (f_{tm} = 2.71 MPa)
Source: own work.

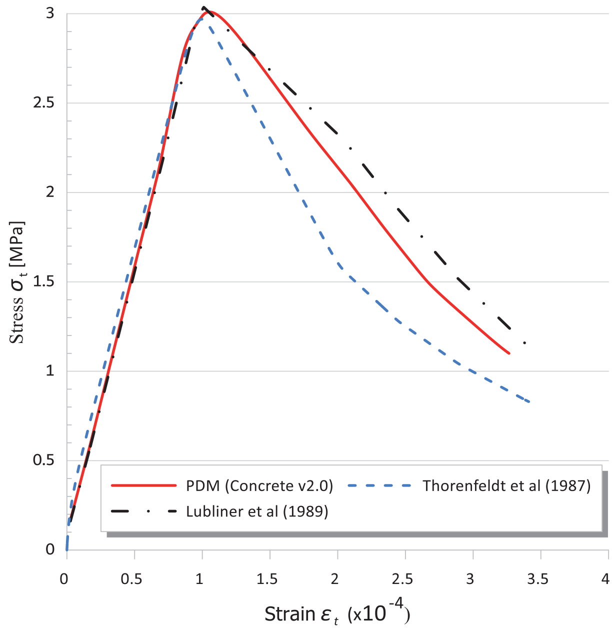

FIGURE 13. Tensile stress–strain curve for f_{cm} = 40 MPa (f_{tm} = 3.04 MPa)
Source: own work.

Conclusions

This paper has provided a comparative study of the stress–strain curves generated according to the Barcelona model and five stress–strain correlations in order to examine the effect of the hardening function in the final outcomes. For the compression case, the outcomes of the Barcelona model were compared with the stress–strain curves of Desayi, Krätzig and Lubliner. The following conclusions can be outlined:

– All curves are relatively close to each other in the ascending part.
– The curves of the Barcelona model are identical to the stress–strain curves generated by the Lubliner's formula.
– For concrete strengths less than 25 MPa, the curves of the Barcelona model are partly consistent with the stress–strain curve generated according to the Krätzig's formula. For values more than 25 MPa, the curves of the Barcelona model move away from the Krätzig's curve depending on the concrete strengths, especially in the descendant part.

– In the descendant part, the difference between the curves of the Barcelona model and of Desayi is significant.

For the tension case, the following conclusions can be made:

– All curves are relatively close to each other in the ascending part.
– The outcomes of the Barcelona model are consistent with the stress–strain curve generated according to the Lubliner's formula.
– The Barcelona model gives results partly similar to the Thorenfeldt's formula, especially in the descendant part.

Consequently, the outcomes of the Barcelona model depend mainly on the hardening function used. In our case, Lubliner's correlations are used as a hardening function in our finite element implementation of DPM (Concrete v. 2.0), which can justify the obtained results. The authors recommend extending the application field of DPM by changing the hardening function (stress–inelastic strain correlation) and re-computing the derivative of the yield function with respect to stresses and the derivative of the yield function with respect to the inelastic compression strain.

References

Ahmed, B., Voyiadjis, G. Z. & Park, T. (2020). Damaged plasticity model for concrete using scalar damage variables with a novel stress decomposition. *International Journal of Solids and Structures*, *191*, 56–75.

Alfarah, B., López-Almansa, F. & Oller, S. (2017). New methodology for calculating damage variables evolution in Plastic Damage Model for RC structures. *Engineering Structures*, *132*, 70–86.

Bakhti, R., Benahmed, B., Laib, A. & Alfach, M. T. (2022). New approach for computing damage parameters evolution in plastic damage model for concrete. *Case Studies in Construction Materials*, *16*, e00834.

Bhartiya, R., Sahoo, D. R. & Verma, A. (2021). Modified damaged plasticity and variable confinement modelling of rectangular CFT columns. *Journal of Constructional Steel Research*, *176*, 106426.

Comité euro-international du béton & Fédération internationale du béton [CEB-FIP] (2010). *Model Code 2010*. London: Thomas Telford.

Desayi, P. & Krishnan, S. (1964). Equation for the stress-strain curve of concrete. *Journal Proceedings*, *61* (3), 345–350.

Dvorkin, E. N., Cuitińo, A. M. & Gioia, G. (1989). A concrete material model based on non-associated plasticity and fracture. *Engineering Computations*, *6*, 281–294.

Han, D. J. & Chen, W. F. (1986). Strain-space plasticity formulation for hardening-softening materials with elastoplastic coupling. *International Journal of Solids and Structures*, *22* (8), 935–950.

Javanmardi, M. R. & Maheri, M. R. (2019). Extended finite element method and anisotropic damage plasticity for modelling crack propagation in concrete. *Finite Elements in Analysis and Design*, *165*, 1–20.

Krätzig, W. B. & Pölling, R. (2004). An elasto-plastic damage model for reinforced concrete with minimum number of material parameters. *Computers & Structures*, *82* (15–16), 1201–1215.

Lee, J. & Fenves, G. L. (1998). Plastic-damage model for cyclic loading of concrete structures. *Journal of Engineering Mechanics*, *124* (8), 892–900.

Liu, Z., Zhang, L., Zhao, L., Wu, Z. & Guo, B. (2022). A damage model of concrete including hysteretic effect under cyclic loading. *Materials*, *15* (14), 5062.

Lu, D., Meng, F., Zhou, X., Wang, G., & Du, X. (2022). Double scalar variables plastic-damage model for concrete. *Journal of Engineering Mechanics*, *148* (2), 1–52.

Lubliner, J., Oliver, J., Oller, S. & Ońate, E. (1989). A plastic-damage model for concrete. *International Journal of Solids and Structures*, *25* (3), 299–326.

Menetrey, P. & Willam, K. J. (1995). Triaxial failure criterion for concrete and its generalization. *Structural Journal*, *92* (3), 311–318.

Meng, H., Yang, W. & Yang, X. (2022). Real-time damage monitoring of double-tube concrete column under axial force. *Arabian Journal for Science and Engineering*, *47*, 12711–12728.

Minh, H. L., Khatir, S., Wahab, M. A. & Cuong-Le, T. (2021). A concrete damage plasticity model for predicting the effects of compressive high-strength concrete under static and dynamic loads. *Journal of Building Engineering*, *44*, 103239.

Oller, S., Ońate, E., Oliver, J. & Lubliner, J. (1990). Finite element nonlinear analysis of concrete structures using a "plastic-damage model". *Engineering Fracture Mechanics*, *35* (1–3), 219–231.

Othman, H. & Marzouk, H. (2018). Applicability of damage plasticity constitutive model for ultra-high performance fibre-reinforced concrete under impact loads. *International Journal of Impact Engineering*, *114*, 20–31.

Ottosen, N. S. (1977). A failure criterion for concrete. *Journal of the Engineering Mechanics Division*, *103* (4), 527–535.

Paliwal, B., Hammi, Y., Moser, R. D., & Horstemeyer, M. F. (2017). A three-invariant cap-plasticity damage model for cementitious materials. *International Journal of Solids and Structures*, *108*, 186–202.

Poliotti, M. & Bairán, J. M. (2019). A new concrete plastic-damage model with an evolutive dilatancy parameter. *Engineering Structures*, *189*, 541–549.

Ren, W., Sneed, L. H., Yang, Y. & He, R. (2015). Numerical simulation of prestressed precast concrete bridge deck panels using damage plasticity model. *International Journal of Concrete Structures and Materials*, *9* (1), 45–54.

Silva, M. A. L., Gamage, J. C. P. H. & Fawzia, S. (2019). Performance of slab-column connections of flat slabs strengthened with carbon fiber reinforced polymers. *Case Studies in Construction Materials*, *11*, e00275.

SIMULIA (2010). *Abaqus analysis user's manual. Volume III: Materials version 6.10*. Vélizy--Villacoublay: Dassault Systémes.

Thorenfeldt, E. (1987). Mechanical properties of high-strength concrete and applications in design. In I. Holand (Ed.), *Utilization of high strength concrete*. Proceedings: symposium in Stavanger, Norway, June 15-18, 1987 (pp. 149–159). Trondheim: Tapir.

Vermeer, P. A. & De Borst, R. (1984). Non-associated plasticity for soils, concrete and rock. *HERON*, *29* (3), 3–64.

Xiao, Y., Chen, Z., Zhou, J., Leng, Y. & Xia, R. (2017). Concrete plastic-damage factor for finite element analysis: Concept, simulation, and experiment. *Advances in Mechanical Engineering*, *9* (9), 1–10.

Summary

Investigation for stress–strain curves of the plastic damage model for concrete. The Barcelona model is one of the most widespread models used in the nonlinear finite element method for simulating the real behavior of concrete. The strong robustness of this model can be attributed to two main reasons, the first one being its ability to account for the elastic stiffness degradation induced by plastic straining and the second one the aptness of considering the stiffness recovery effects under cyclic loading. This model was examined in the paper by comparing the generated stress–strain diagrams with several analytical solutions from the literature. The comparing process in the compression and tension cases with the closed-form solutions of Desayi, Krätzig, Lubliner and Thorenfeldt proved that the Barcelona model provided identical outcomes with Lubliner's formula, which was used as the hardening function in the finite element implementation of this model. What is more, this model provided the same curves in case of the others in the ascending branches, and for the descending branch, this study proved that the outcomes of the Barcelona model are completely different from the ones of Desayi in the compression case and slightly similar to Thorenfeldt's curves in the tension case.